



UNIVERSITÀ DI PISA



Commissioning of the Mu2e tracker DAQ, planning for the Vertical Slice Test and pre-pattern recognition studies

Candidate:

Sara Gamba

Supervisors:

Pavel Murat (FNAL)

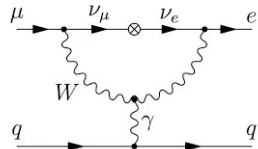
Simone Donati (Unipi, INFN Pisa)

October 21st 2024

Charged Lepton Flavour Violation

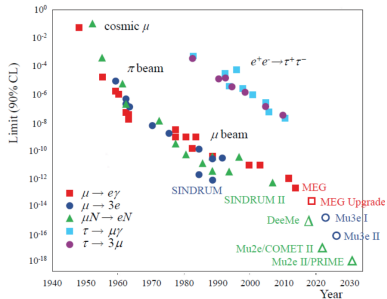
- The **Standard Model** (SM) does not predict lepton flavour violation;
- The discovery of **neutrino oscillations** prove that lepton interactions are non-diagonal in flavour;
- The SM fails to explain phenomena like neutrino masses and the consequent flavour oscillations;
- The branching ratios of **CLFV** processes, including neutrino oscillations, are suppressed by factors proportional to $(\Delta m_\nu^2)^2/M_W^4$ and expected to be less than $\mathcal{O}(10^{-50})$;
- This value is far beyond current experimental capabilities.

| QUARKS | | |
|----------------------------------|----------------|-------------------------|
| mass $=2.2 \text{ MeV}/c^2$ | $\frac{2}{3}$ | $\frac{1}{2}$ |
| charge $\frac{2}{3}$ | $\frac{2}{3}$ | $\frac{1}{2}$ |
| spin $\frac{1}{2}$ | $\frac{1}{2}$ | $\frac{1}{2}$ |
| u | c | t |
| up | charm | top |
| mass $=4.7 \text{ MeV}/c^2$ | $\frac{1}{3}$ | $\frac{1}{2}$ |
| charge $-\frac{1}{3}$ | $-\frac{1}{3}$ | $-\frac{1}{2}$ |
| d | s | b |
| down | strange | bottom |
| mass $=0.5 \text{ MeV}/c^2$ | -1 | -1 |
| charge -1 | -1 | -1 |
| e | μ | τ |
| electron | muon | tau |
| mass $=0.511 \text{ MeV}/c^2$ | $\frac{1}{2}$ | $\frac{1}{2}$ |
| charge 0 | 0 | 0 |
| ν_e | ν_μ | ν_τ |
| electron neutrino | muon neutrino | tau neutrino |
| LEPTONS | | |
| mass $<1.0 \text{ eV}/c^2$ | 0 | $<18.2 \text{ MeV}/c^2$ |
| charge 0 | 0 | 0 |
| ν_e | ν_μ | ν_τ |
| electron neutrino | muon neutrino | tau neutrino |



Search for CLFV

- ▶ New Physics (NP) models predict much higher rates of CLFV;
- ▶ Observing CLFV would provide unambiguous evidence of **physics beyond the SM**;
- ▶ CLFV channels involving muons:
 $\mu^+ \rightarrow e^+ \gamma$, $\mu^- N \rightarrow e^- N$ and
 $\mu^+ \rightarrow e^+ e^+ e^-$;
- ▶ $\mu^- N \rightarrow e^- N$ channel:
 - Higher momentum signal and better separation from the background;
 - Benefits from high intensity beam;
 - Better sensitivity to CLFV in a large range of NP scenarios.
- ▶ Current best limit on $\mu^- N \rightarrow e^- N$ by SINDRUM II: $R_{\mu e} < 7 \times 10^{-13}$ (90% CL).



The Mu2e experiment

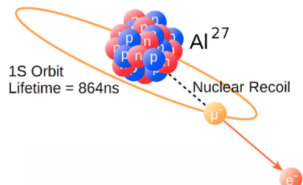
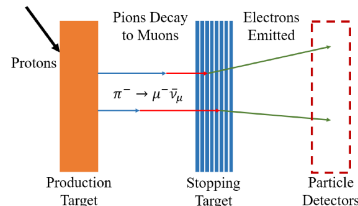
- ▶ Search for neutrinoless, coherent conversion $\mu^- N \rightarrow e^- N$ in the field of an Al nucleus, by measuring:

$$R_{\mu e} = \frac{\mu^- + N(Z, A) \rightarrow e^- + N(Z, A)}{\mu^- + N(Z, A) \rightarrow \nu_\mu + N(Z - 1, A)}$$

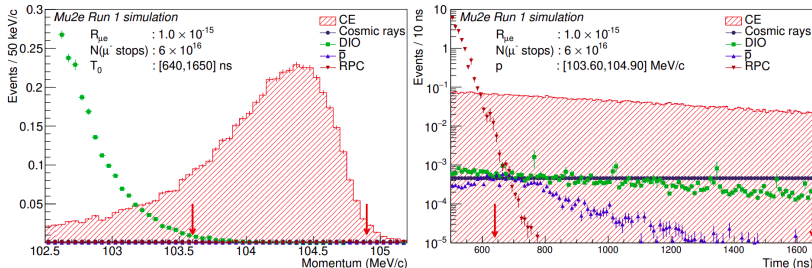
- ▶ Mu2e goal is to improve SINDRUM II limit by 4 orders of magnitude;
- ▶ The signal is a monochromatic conversion electron (CE) with energy:

$$E_{CE} = m_\mu - E_{recoil} - E_{bind} = 104.97 \text{ MeV}$$

where m_μ is the muon mass, E_{recoil} the target nucleus recoil energy and E_{bind} the muonic atom $1s$ state binding energy.

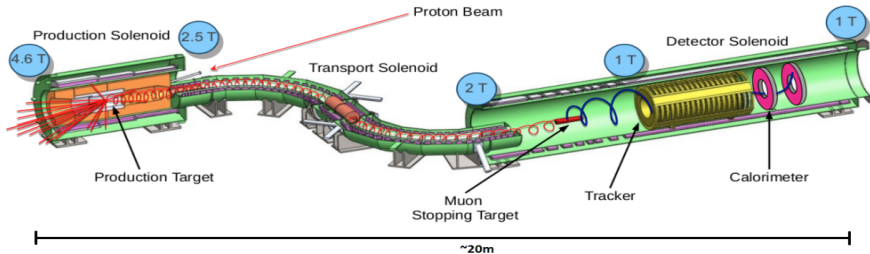


Background sources



- ▶ **Cosmics** → veto enclosing the detector (≈ 0.046 evs/RunI);
- ▶ **Intrinsic** → 1 MeV/c momentum resolution:
 - Decay In Orbit $\mu^- N \rightarrow e^- \bar{\nu}_e \nu_\mu N$ (≈ 0.038 evs/RunI);
 - Radiative Muon Capture $\mu^- N \rightarrow \gamma \nu_\mu N'^*$ (< 0.0024 evs/RunI).
- ▶ **Delayed processes from \bar{p}** → absorbers in the TS (≈ 0.010 evs/RunI);
- ▶ **Prompt processes** → pulsed beam + delayed live window:
 - Radiative Pion Capture $\pi^- N \rightarrow \gamma N'^*$ (≈ 0.010 evs/RunI);
 - π and μ Decay In Flight ($< 2 \times 10^{-3}$ evs/RunI);
 - Beam electrons ($< 1 \times 10^{-3}$ evs/RunI).

The Mu2e experimental setup



► Production Solenoid:

- 8 GeV pulsed proton beam interacts with the W target and mostly π s are produced;
- graded field for backward collection.

► Transport Solenoid:

- it allows for π decay and μ transport;
- *S*-shape for charged particle selection;
- it selects muons with $p \lesssim 100$ MeV/c;
- rotating collimator COL3 selects μ^- or μ^+ beam.

► Detector Solenoid: Stopping Target, p absorber and detectors.

The electromagnetic calorimeter

Calorimeter is vital for:

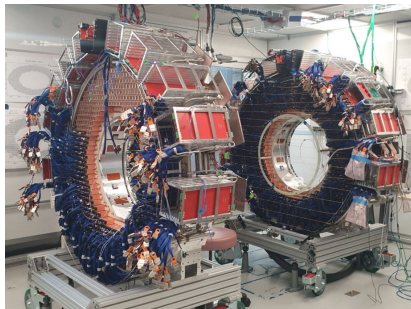
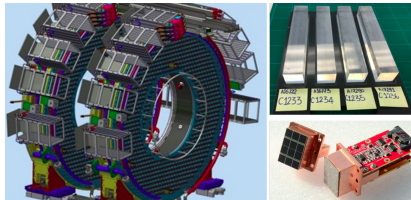
- ▶ **PID (E/p);**
- ▶ Seed for **track reconstruction;**
- ▶ Fast online **trigger filter.**

Design:

- ▶ 2 hollow disks of crystals, 70 cm apart;
- ▶ 2×674 CsI crystals per disk, each coupled to 2 SiPMs.

Performance:

- ▶ $\sigma_E/E \sim 10\%$;
- ▶ $\sigma_{xy} \sim 6$ mm;
- ▶ $\Delta t < 500$ ps.



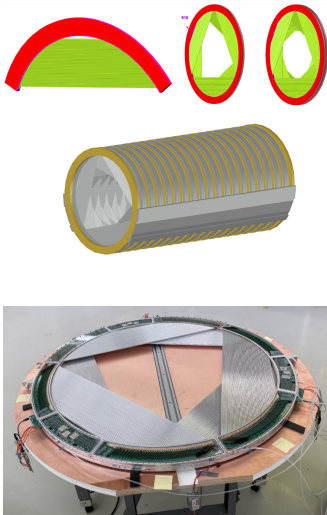
The straw tracker

Purpose:

- ▶ momentum measurement with $\Delta p < 300 \text{ keV}/c \text{ FWHM} + 950 \text{ keV}/c$ energy losses (ST and proton absorber) (DIO).

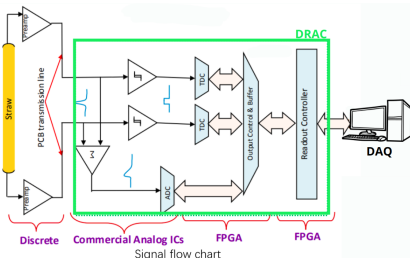
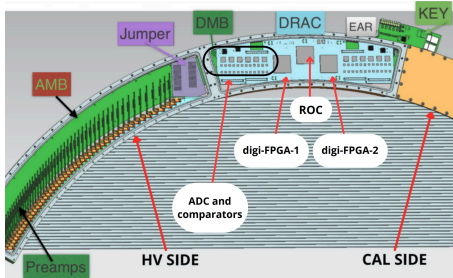
Design:

- ▶ 3 m downstream of the ST ($B \sim 1 \text{ T}$);
- ▶ hollow geometry (low p_T particles);
- ▶ 3 m long tracker in vacuum;
- ▶ 96 straws per panel, 6 panels per plane, 2 planes per station;
- ▶ 18 tracking stations: 216 panels;
- ▶ 5 mm diameter and 40-110 cm long straws filled with a 80%:20% Ar:CO₂ mixture at a pressure of 1 atm.



The tracker readout and DAQ

- ▶ Signal is readout from both ends by **preamps** (**CAL** and **HV** side);
- ▶ Analog signals are sent to the **DRAC** (Digitizer Readout & Assembler Controller) and processed by 2 **TDCs** and one **ADC**;
- ▶ The 2 **digi-FPGA** create one data packet for each hit containing the **two hit times** and **one waveform**;
- ▶ Data packets are transferred to the **ROC** (Readout Controller);
- ▶ ROC collects, buffer and transfer data from digi-FPGAs to **DTC** (Data Transfer Controller) installed on **DAQ** computers;
- ▶ DTC sends data request to the ROC and data from DTC is sent to the Event Builder.



My Thesis

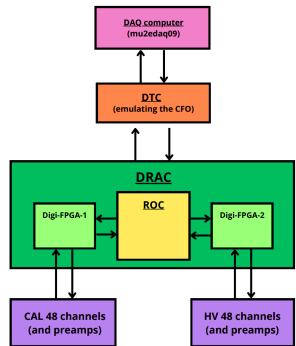
- ▶ Mu2e is starting detector **commissioning** and **calibration**;
- ▶ My work consists of a **comprehensive study of the Mu2e tracker**:
 - **Vertical Slice Test (VST)**. The entire testing chain, from the straws to the readout, to processed data on disk:
 - ▶ initial tracker **DAQ** and **FEE** testing;
 - ▶ validation of the **ROC** readout and buffering;
 - ▶ study of tracker **preamps** performance.
 - First steps towards the tracker timing **calibration** with **cosmics**:
 - ▶ determine **signal propagation** and **channel-to-channel delay**;
 - ▶ develop an **unbiased cosmic track reconstruction** procedure.
 - **Mu2e Offline**. Pre-pattern recognition studies:
 - ▶ estimated data volume for Mu2e data-taking is **>7 PBytes/year**;
 - ▶ the **primary source** of hits in the Mu2e tracker will be δ -electrons;
 - ▶ important to identify those hits without losing **CE efficiency**.

Outline

- ▶ Commissioning of the tracker DAQ and FEE:
 - validation of ROC readout;
 - study of preamplifiers performance.
- ▶ First steps towards the station calibration;
- ▶ Pre-pattern recognition studies;
- ▶ Conclusions.

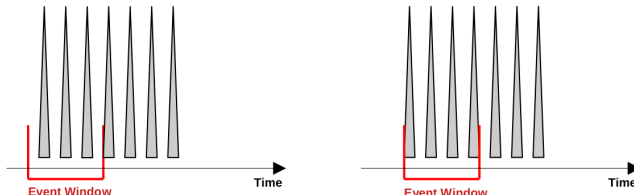
Description of test stand setup

- ▶ ROC readout validation;
- ▶ TS1 tracker test stand: one DTC connected to the DAQ computer, one ROC (one tracker panel-96 channels);
- ▶ ROC can be operated in two different data readout modes:
 - MODE 1: emulated data readout mode;
 - MODE 2: digi-FPGA readout mode.
- ▶ digi-FPGAs pulsed by their **internal pulser** at $f_{gen} = 250$ kHz or 60 kHz;
- ▶ **Event Window (T_{EW})**: the time interval between two proton pulses, varied between 700 ns to 50 μ s;
- ▶ The ROC firmware has an internal **hit buffer** which stores up to **255 hits**.



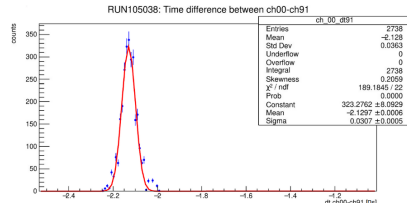
Logic of data taking

- ▶ Depending on $T_{gen} = 1/f_{gen}$ and T_{EW} , the data taking can proceed in two different modes:
 - $N_{gen} \geq 255$: $N_{readout} = 255$;
 - $N_{gen} < 255$: $N_{readout} < 255$;
- ▶ Each FPGA has its own generator and pulses from different generators are offset ($\in [0, T_{gen}]$) with respect to each other;
- ▶ Timing of generator pulses uncorrelated with the beginning of the EW
→ different number of hits in an EW;
- ▶ Offsets between channels (same digi-FPGA) are about few ns and can be measured;
- ▶ Channel readout sequence is fixed.



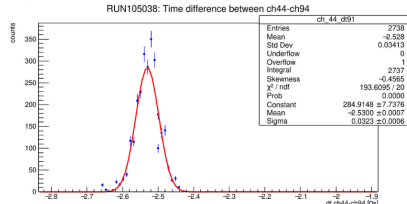
Monte Carlo simulation

- ROC readout logic emulated with a bit-level C++ simulation;
- Simulated parameters:
 - number of hits in each channel;
 - number of readout hits per event.
- digi-FPGAs and channel to channel offsets considered.

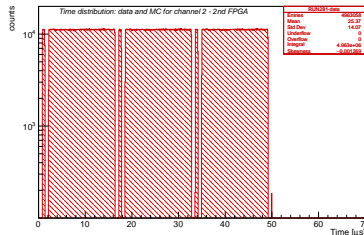
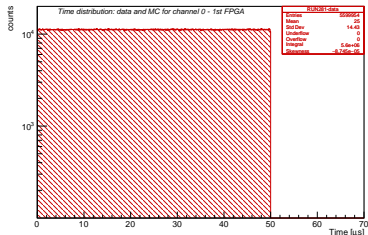


Steps of the simulation:

- EW starts at $t = 0$ s;
- The 1st pulse is generated $T_0 \in [0, T_{gen}]$;
- Next pulses: $T_i = T_{i-1} + T_{gen}$, until $T_i > T_{EW}$;
- Pulses are generated in each channel following the readout sequence;
- The procedure *continues* until all hits have been *readout*, or $N_{hits} > 255$.



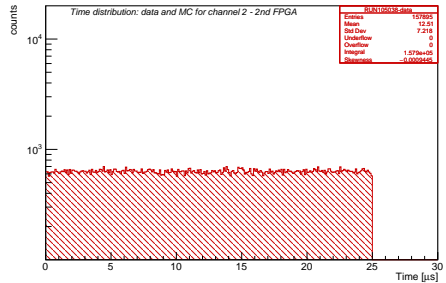
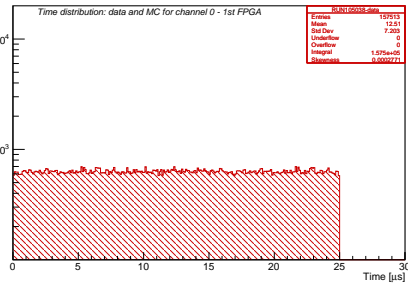
Hit timing distribution: overflow mode



- ▶ The distribution of the hit time for channel 0 of digi-FPGA-1 (Left) and channel 2 of digi-FPGA-2 (Right);
- ▶ $T_{EW} = 50 \mu\text{s}$ and $f_{gen} = 60 \text{ kHz}$;
- ▶ Left distribution is uniform, Right one is non-trivial;
- ▶ Different behaviour for different channels in different FPGAs;
- ▶ Apparently there are interruptions of channel 2 in the second FPGA;
- ▶ Everything can be explained with the *occupancy* plot.

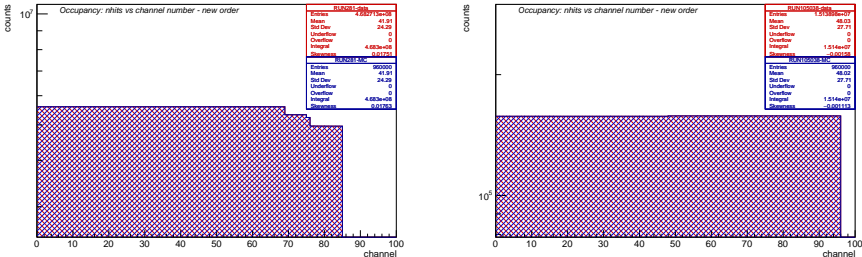
Hit timing distribution: regular mode

counts



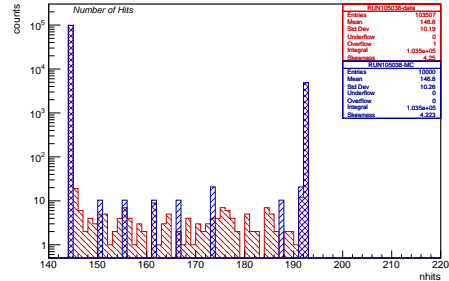
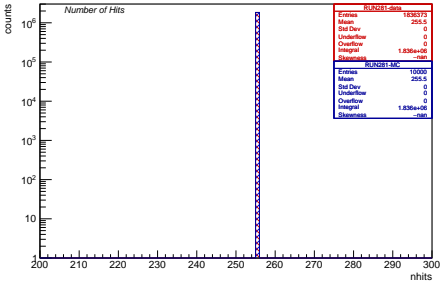
- The distribution of the hit time for channel 0 of digi-FPGA-1 (Left) and channel 2 of digi-FPGA-2 (Right);
- $T_{EW} = 25 \mu\text{s}$ and $f_{gen} = 60 \text{ kHz}$;
- Same behaviour for different channels in different FPGAs;
- No interruptions of channel 2 in the second FPGA.

Occupancy plots



- ▶ Occupancy plot: number of hits versus channel number (data red, MC blue);
- ▶ The bin ordering corresponds to the channel readout ordering;
- ▶ Overflow mode (Left):
 - channels 0-68: 48 digi-FPGA-1 channels with 4 hits (192 hits) and 21 digi-FPGA-2 channels with 3 hits (63 hits);
 - channels 0-75: 48 digi-FPGA-1 channels with 3 hits (144 hits) and 27 digi-FPGA-2 channels with 4 hits (108 hits) and 1 with 3 hits (111 hits);
 - channels 0-85: 48 digi-FPGA-1 channels with 3 hits (144 hits) and 37 digi-FPGA-2 channels with 3 hits (111 hits).
- ▶ Regular mode (Right): all channels with same occupancy ($N_{hits} < 255$).

Number of hits distribution



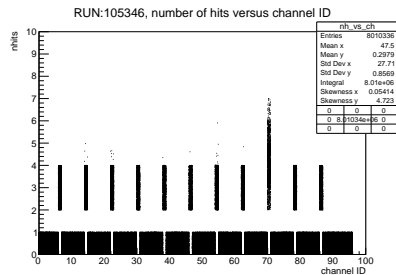
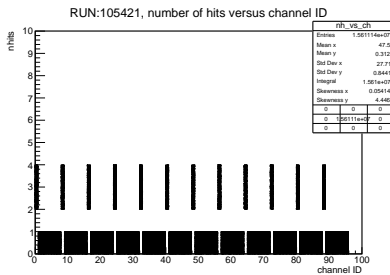
- ▶ Overflow mode (Left): distribution of number of hits peaked in 255;
- ▶ Regular mode (Right): the number of hits distribution depends on the relative offset of the EW with respect to the digi-FPGA pulsers and it varies from 144 to 192;
- ▶ Agreement between MC and data at a level of 10^{-3} .

Outline

- ▶ Commissioning of the tracker DAQ and FEE:
 - validation of ROC readout;
 - study of preamplifiers performance.
- ▶ First steps towards the station calibration;
- ▶ Pre-pattern recognition studies;
- ▶ Conclusions.

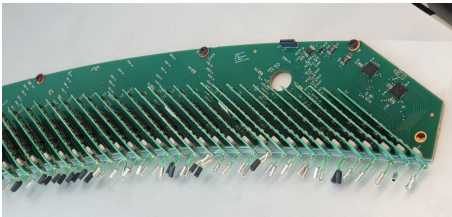
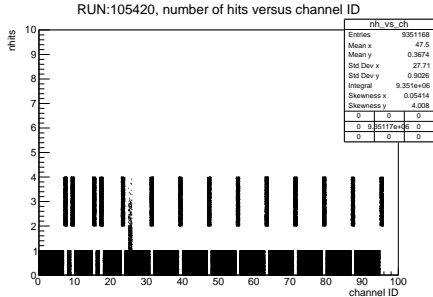
Test 1: channel occupancy versus channel ID

- ▶ Same test stand: 1 or 2 ROCs and one DTC, plus preamps on the CAL side;
- ▶ CAL side digi-FPGA generates calibration pulses, pulsing every 8th channel across 12 RUNs (different starting channel);
- ▶ The frequency was set to 50 kHz and $T_{EW} = 50 \mu\text{s}$, 2 or 3 hits per channel;
- ▶ Looking for cross talks, non-uniform occupancy, dead channels.



- ▶ (Left): regular occupancy;
- ▶ (Right): 94th channel dead (preamp substituted) and $N_{hits} > 3$ in some channels → time distribution and inverted waveforms in Test 2.

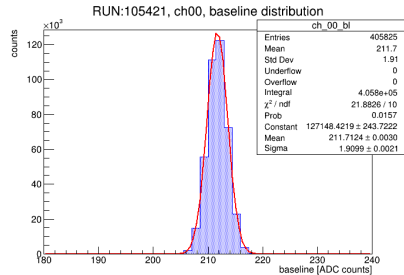
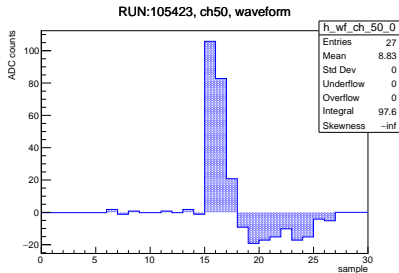
Test 1: channel occupancy versus channel ID



- ▶ (Left): occupancy plot with cross talks in first odd channels and only asymmetric (e.g. $3 \rightarrow 5$, not seen $3 \rightarrow 1$);
- ▶ (Right): preamp boards are mounted vertically and odd channels are those on the PCB board;
- ▶ The distance between the first channels is slightly lower;
- ▶ The solution to these cross talks is still object of study.

Test 2: analysis of the readout pulses waveforms

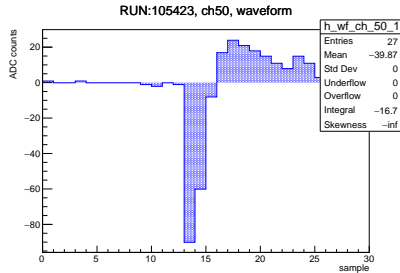
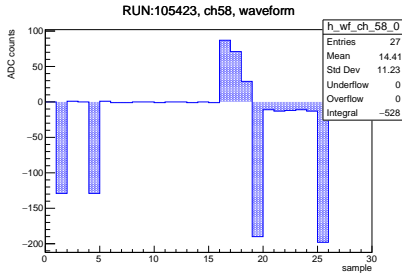
- ▶ Same test stand;
- ▶ Checking signal uniformity among channels within the same ROC or across multiple ROCs, and among different events;
- ▶ 40 MHz ADC (25 ns sample width) and pulser frequency set to 50 kHz.



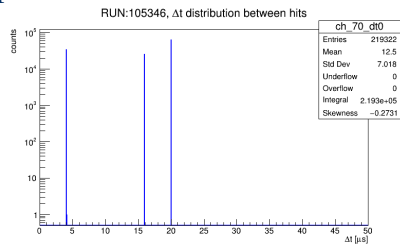
- ▶ (Left): regular waveform;
- ▶ Flat distribution in the first 10 samples (baseline), high positive charge peak with a sharp leading edge, negative tail;
- ▶ (Right): fitted baseline distribution, with mean at 210 ADC counts and $\text{FWHM} = 2\sqrt{2\ln 2}\sigma \sim 4.5$ ADC counts.

Test 2: analysis of the readout pulses waveforms

- Different baseline values indicating noise, dips, inverted waveforms.

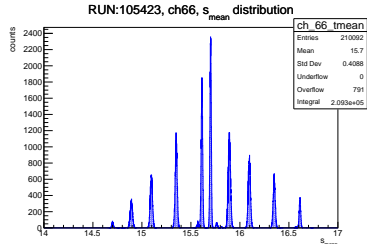
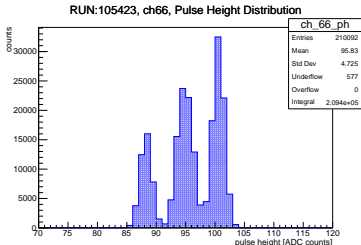


- (Left): dips of specific depths (64, 128 or 192) → ADC 6th or 7th bits;
- Problematic samples identified and excluded from the baseline estimate;
- (Right): inverted waveform → Δt distribution peaked in $16 \mu\text{s}$ (regular) and $4 \mu\text{s}$ (inverted). Trigger on trailing edge of $4 \mu\text{s}$ long input pulses.

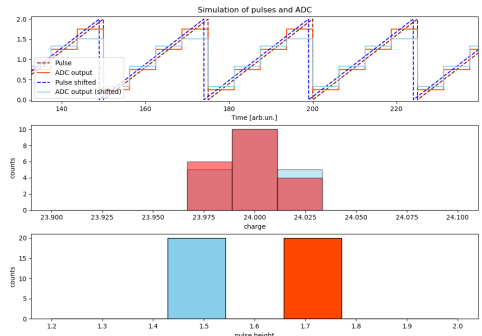


Test 2: analysis of the readout pulses waveforms

- (Left): pulse height (PH) (charge) distribution with 2/3 peaks.

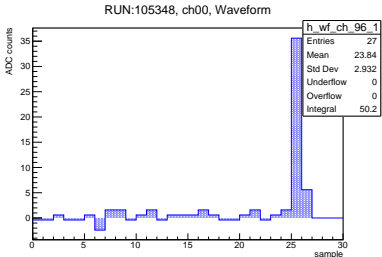
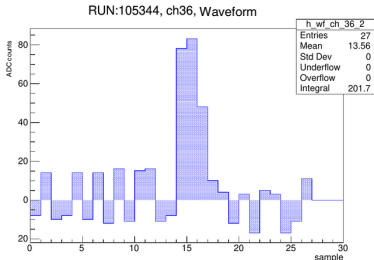


- (Top Right): $s_{\text{mean}} = \frac{\sum_i \text{sample}_i \cdot q_i}{\sum_i q_i}$ distribution, correlated with PH (charge) peaks;
- (Bottom Right): simulation of the charge and PH distribution behaviour;
- This is an artifact of the pulser timing shifted with respect to the ADC clock of few ns.

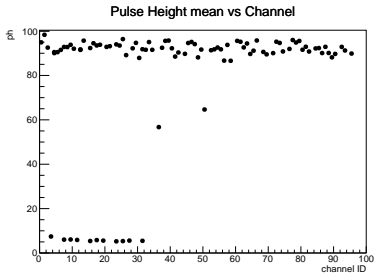
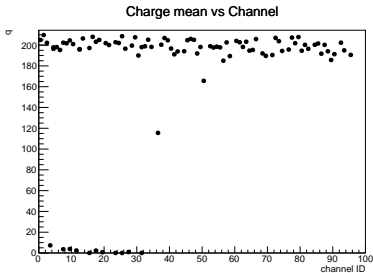


Test 2: analysis of the readout pulses waveforms

- ▶ Charge distribution used to check noisy channels (Left) and glitches (Right).



- ▶ Check of the response uniformity across channels.

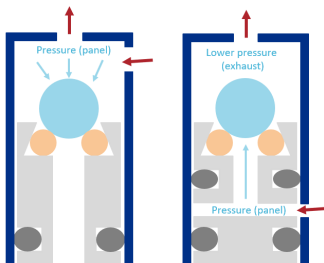


Outline

- ▶ Commissioning of the tracker DAQ and FEE:
 - validation of ROC readout;
 - study of preamplifiers performance.
- ▶ First steps towards the station calibration;
- ▶ Pre-pattern recognition studies;
- ▶ Conclusions.

First steps towards the station calibration

- ▶ **Calibration goal:** straw longitudinal position resolution $\lesssim 4$ cm;
- ▶ TDCs measure arrival times t_1 and t_2 ;
- ▶ v : signal propagation velocity;
- ▶ x_{track} : reconstructed track position along the wire;
- ▶ t_0 particle crossing, t_d drift time, L straw length, d_i delays by FEE;
- ▶ **Calibration:** v from Δt_{12} (TDCs) correlated with x_{track} (**unbiased**);
- ▶ x_{track} determined by straw "yes or no" information → **station geometry**.

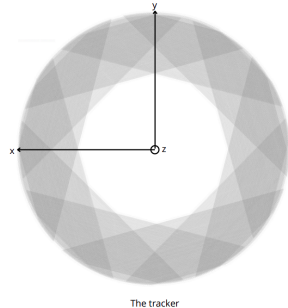


- ▶ First calibration with **cosmics**;
- ▶ Unbiased reconstruction with *horizontal orientation*;
- ▶ **Operational constraints:** gas system (sealing with vertical valves), space, fragility. Designed to be operated **vertically**;
- ▶ **Simulation with vertical station to assess biases and feasibility.**

Monte Carlo muon selection and reconstruction

► Cosmics as calibration source:

- standard detector operations;
- flux is $\sim 1 \text{ cm}^{-2}\text{min}^{-1}$ (for horizontal detectors) and $E_{mean} \sim \text{GeV}$;
- MIP;
- $v_\mu \sim c \rightarrow$ align channel offsets.



► Straw information:

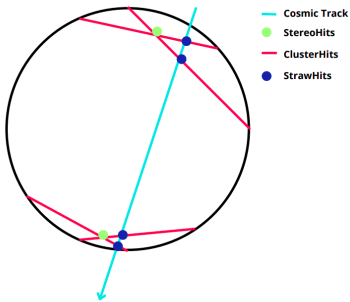
- the direction ($D_{x,i}, D_{y,i}$);
- the midpoint ($M_{x,i}, M_{y,i}$);
- the z_i coordinate.

► Selection:

- Hits in **one vertical station**;
- **Straight line in 3D**: ≥ 4 hits at different $z \rightarrow nhits_{face_i} \geq 1$;
- **Resolution**: $nhits_{panel_i} \leq 3$.

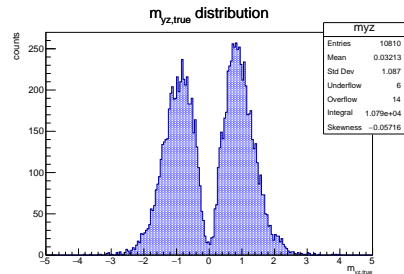
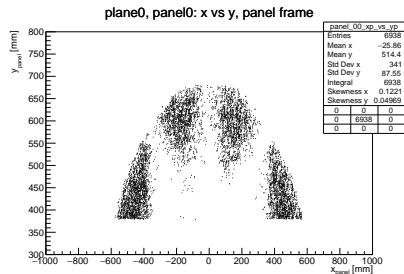
► Reconstruction:

- $StrawHits \rightarrow 1 ClusterHit$ (face);
- $2 ClusterHits \rightarrow StereoHit$ (plane);
- $2 StereoHits \rightarrow$ reconstructed track.



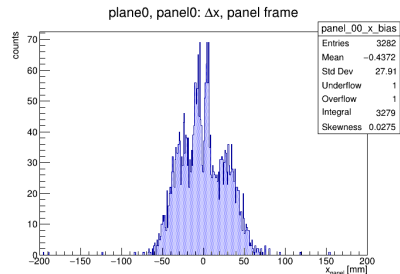
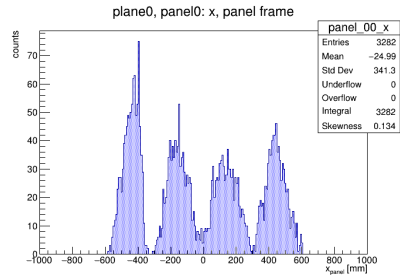
Panel illumination pattern and muon directions

- ▶ Precise calibration: uniformly distributed hits across the panel;
- ▶ (Top): muon selections bring to **non uniform** and spotty panel illumination;
- ▶ 4/4 overlap areas limited to **panel edges**;
- ▶ **Waveform non-linearities**;
- ▶ Selection of **specific muon directions**;
- ▶ (Bottom): $m_{yz} = \Delta y / \Delta z$ distribution;
- ▶ No particles with $m_{yz} \sim 0$ (horizontal) and $m_{yz} \rightarrow \infty$ (vertical);
- ▶ Mostly with $|m_{yz}| \sim 1$ (**45° angle**);
- ▶ Muon **rate** scaled by $1 / \cos^2 \theta \sim 1/2$ (45° flux) and $1/\sqrt{2}$ (cosmics striking at 45°).



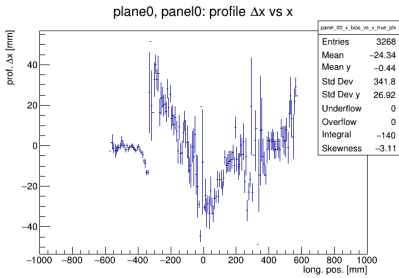
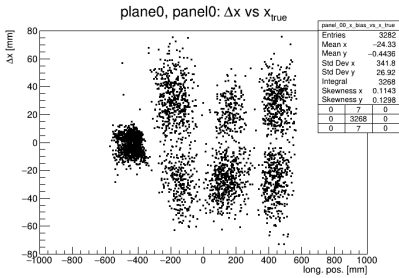
Longitudinal position reconstruction

- (Top): longitudinal reconstructed position x_{track} (panel frame);
- x_{track} : intersection of the reconstructed track with the mean z_i of the panel;
- **Bumps** \rightarrow 4/4 requirement consequence;
- Different bumps \rightarrow different straws;
- (Bottom): longitudinal reconstructed position **bias** (panel frame);
- $\Delta x = x_{track} - x_{true}$;
- x_{true} : MC panel hits mean coordinate;
- The bias ranges between [-6,6] cm;
- Similar distributions for all panels;
- Different straws with different bias;
- $m_{yz} = \frac{\Delta y}{\Delta z}$ not accurately reconstructed.



Results

- (Top): 2D distribution of Δx vs x_{true} ;
- Different spots → different overlap regions and muon directions;
- (Bottom): Δx profile vs x_{true} ;
- x_{track} reconstruction systematics ± 4 cm;
- $m_{yz} = \frac{\Delta y}{\Delta z}$ not accurately reconstructed;
- Vertical station: **opposite $y - z$ orientated muons do not cancel out**;
- First spots: 90° panels overlap;
- **Increase of data-taking time**;
- **This calibration is expected to become challenging.**



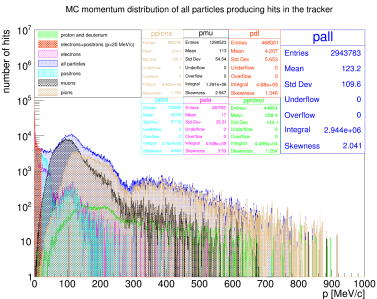
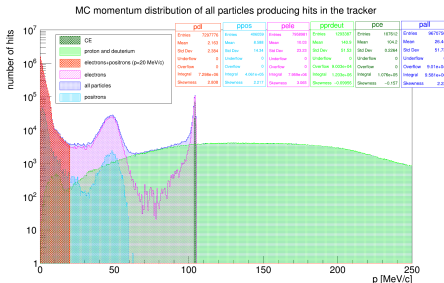
Outline

- ▶ Commissioning of the tracker DAQ and FEE:
 - validation of ROC readout;
 - study of preamplifiers performance.
- ▶ First steps towards the station calibration;
- ▶ Pre-pattern recognition studies;
- ▶ Conclusions.

Introduction

- ▶ Most of **tracker hits** are e^- and e^+ with $E < 20 \text{ MeV}$ - **δ -electrons**:
 - **Compton scattering**: interaction of γ s (n capture) with material;
 - **e^\pm pairs**: nuclear recoil processes;
 - **δ -rays**: interaction of high-energy charged particles with material.
- ▶ Mu2e data: $\geq 7 \text{ PB/year} \rightarrow \text{CPU optimization critical}$;
- ▶ Hit flagging to avoid sending them to pattern recognition;
- ▶ Crucial step for several **physics reasons**:
 - **CE track reconstruction efficiency**;
 - **Protons**: complementary source to determine muon stopping rate;
 - **\bar{p} background**: correct background estimate.
- ▶ Data-sample:
 - **CE-1BB**: CE signal + pileup ($1\text{BB}-1.6 \times 10^7$ protons/pulse);
 - **CE-2BB**: CE signal + pileup ($2\text{BB}-3.9 \times 10^7$ protons/pulse);
 - **PBAR-0BB**: $\bar{p}s$ and no pileup.

δ -electrons in Mu2e tracker

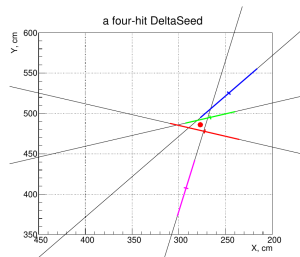
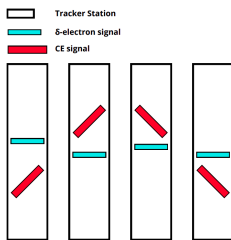


- Momentum distribution of particles making at least one hit in the tracker (Left: **CE-1BB**, Right: **PBAR-0BB**) (blue) all particles, (orange) δ s, (green) p and D , (pink) e^- , (cyan) e^+ , (dark green) CE, (black) μ , (beige) π ;
- (Left): 75% of hits by δ -electrons (71% e^- , 4% e^+ - Compton scattering);
- (Left): bump in the e^+ distribution ($N(\mu^+ \rightarrow e^+)/N(\mu^- \rightarrow e^-) \sim 10^{-3}$ for μ entering the DS and DIO on IPA should be also 10^{-3} wrt μ^- DIF);
- (Right): $p\bar{p}$ annihilation in ST \rightarrow multiple tracks with $p \sim 100/200$ MeV/c;
- Reconstructing these tracks helps constrain background.

δ -electrons flagging algorithms

Two pre-pattern recognition algorithms developed in Mu2e Offline:

- ▶ **FlagBkgHits (FBH).** First it finds clusters of hits close in $x - y$ and time and uses an ANN to classify them. Based on *StereoHit* reconstruction;
- ▶ **DeltaFinder (DF).** Search for hit patterns consistent with δ -electron ones:
 - δ segments in each station (*seed*, 3 or 4 hits cluster in space and time);
 - straws intersection determined \rightarrow center of gravity on $x-y$;
 - *seeds* close in $x-y$ and time across stations connected (δ candidate);
 - p candidates (*seeds* with $\bar{E}_{dep} > 3$ keV).



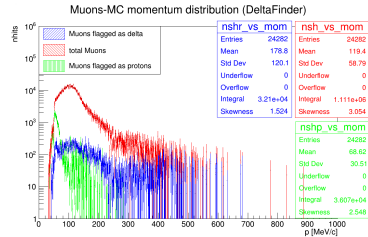
- ▶ (Left): δ -electrons and CE patterns in the $r - z$ plane;
- ▶ (Right): A δ candidate *seed*.

Performance analysis and comparison

Two levels of comparison:

- **hit-level:** how accurately individual hits are flagged (most direct method);
- **high-level:** reconstruction level comparison (figure of merit: CE tracks).
- Before comparing: **proton hit flagging over-efficiency by DF.**

| | f_p | f_e |
|-------|-------|-------|
| p | 96.0% | 1.0% |
| μ | 5.8% | 5.0% |
| π | 2.5% | 11.2% |



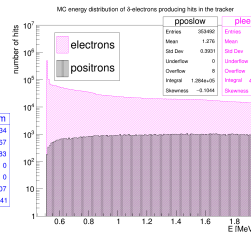
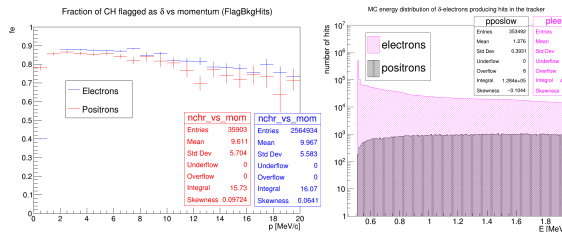
- (Left): f_p and $f_e \rightarrow$ fraction of hits flagged as p and e^- ;
- (Right): distribution of the total (red) and flagged (green) number of μ hits as a function of the particle momentum;
- High μ and π $f_p \rightarrow$ low momentum (higher energy deposition as p);
- *Good* proton candidate $\rightarrow \geq 4$ hits with $E_{dep} > 3$ keV;
- ϵ_p reduced of 10%, but μ and π f_p reduced by factor of 2 and 6 \rightarrow next slide.

Hit-level comparison

- (Top Tab): **PBAR.** μ and π $f_{p,FBH}$ 4x and 3.3x higher;
- FBH: **supervised training** with CE+pileup dataset;
- π : higher momenta \rightarrow smaller curvature \rightarrow higher f_e ;
- (Bottom Tab): **CE-1BB**. Same results for **CE-2BB** within 1%;
- **70% more CE hits flagged** as δ -electrons by FBH with respect to DF;
- **No p flagging comparison** (FBH identifies only high E_{dep} particles).

| | f_p DF | f_e FBH | f_e DF |
|-------|----------|-----------|----------|
| μ | 2.7% | 13.0% | 3.2% |
| π | 0.4% | 23.8% | 7.3% |

| | f_p DF | f_e FBH | f_e DF |
|----------------------|----------|-----------|----------|
| $e^- < 20$ MeV/c | 2.5% | 75.9% | 72.5% |
| $e^- [20,80]$ MeV/c | 1.0% | 50.0% | 27.4% |
| $e^- [80,110]$ MeV/c | 0.3% | 5.7% | 3.4% |
| p | 83.7% | | 1.0% |
| $e^+ < 20$ MeV/c | 0.2% | 85.5% | 88.5% |



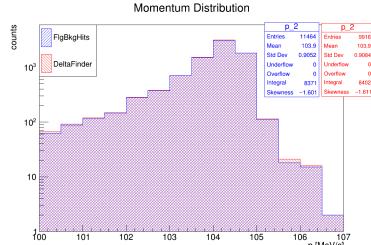
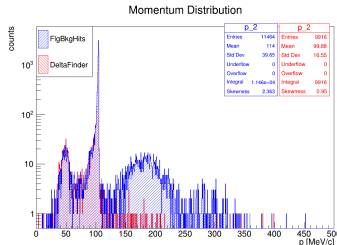
- (Left): e^- and e^+ f_e vs momentum (FBH);
- 1-2 MeV: δs with 1/2 hits per station (DF>3hits);
- >2 MeV: larger xy spread;
- (Right): e^- (pink) and e^+ (black, no Compton) E distribution ($E < 2$ MeV).

High-level comparison

- (Top Tab): **PBAR**. DF has 22% advantage in reconstructing 2 tracks (hit-level);
- 80 MeV/c cut: minimum reconstructable particle p from ST in the tracker;
- 90 MeV/c cut: DIO suppression;
- (Bottom Tab): **CE-1BB**. Same CE reconstruction efficiency (the hit-level difference is 1 hit/track);
- FBH (blue) & DF (red) reconstructed tracks p distributions (two ranges);
- FBH flags less proton hits and these hits are sent to pattern recognition.

| fraction of events | FBH | DF |
|---|------|------|
| $N_{tracks} \geq 2$ | 1.8% | 2.2% |
| $N_{tracks} \geq 2 \text{ & } p > 80 \text{ MeV/c}$ | 1.7% | 2.1% |
| $N_{tracks} \geq 2 \text{ & } p > 90 \text{ MeV/c}$ | 1.6% | 2.0% |

| | FBH | DF |
|---------------------------------|-------|-------|
| CE events with $N_{tracks} > 0$ | 37.9% | 37.9% |



Outline

- ▶ Commissioning of the tracker DAQ and FEE:
 - validation of ROC readout;
 - study of preamplifiers performance.
- ▶ First steps towards the station calibration;
- ▶ Pre-pattern recognition studies;
- ▶ Conclusions.

Conclusions

- CLFV processes provide a clean test field for **NP models**;
- Mu2e is one of the leading experiments and searches for $\mu^- N \rightarrow e^- N$;
- Mu2e success depends on the performance of the **tracker**;
- **Comprehensive study** from the tracker readout to offline analysis:
 - DAQ and FEE testing:
 - **ROC readout validation** with MC at a level of 10^{-3} ;
 - **Preamps performance study**: dead channels, cross-talk between the channels, and waveform patterns study.
 - First steps towards timing calibration:
 - **Vertical station orientation** → non-uniform panel illumination;
 - Large **bias** on x_{track} reconstruction (± 4 cm);
 - Increase of data-taking time;
 - Pre-pattern recognition study to flag δ -electrons:
 - **Hit-level**: FBH flags 70% more CE hits, same performance for δ s, no possible p flag comparison, FBH not trained one \bar{p} data sample;
 - **High-level**: same reconstruction performance for CE signal;
 - **Timing**: 0.13, 0.39 ms/ev (1BB, 2BB) more for DF vs 5 ms/ev expected;
 - **Important to improve TimeCluster efficiency**.

Thank you for your attention!

Bibliography

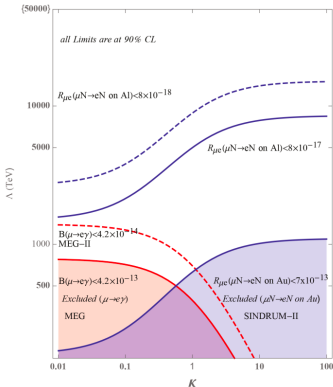
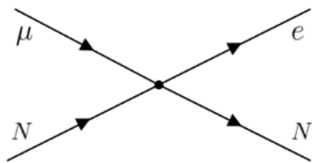
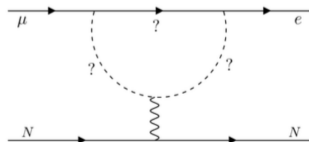
- [1] BERNSTEIN, R.H. AND COOPER, PETER S., *Charged lepton flavor violation: An experimenter's guide*, Physics Reports, 532 (2013), pp. 27–64.
- [2] BERNSTEIN, ROBERT H., *The Mu2e Experiment*, Frontiers in Physics, 7 (2019).
- [3] M. COLLABORATION, *Mu2e Run I Sensitivity Projections for the Neutrinoless $\mu^- \rightarrow e^-$ Conversion Search in Aluminum*, Universe, 9 (2023).
- [4] H. KOLANOSKI, N. WERMES, *Particle detectors*, Oxford University Press, 2020.
- [5] KARGIANTOULAKIS, MANOLIS, *A search for charged lepton flavor violation in the Mu2e experiment*, Modern Physics Letters A, 35 (2020), p. 2030007.
- [6] L. CABIBBI, G. SIGNORELLI, *Charged Lepton Flavour Violation: An Experimental and Theoretical Introduction*, La Rivista del Nuovo Cimento, 41 (2018), pp. 71–174.
- [7] MU2E COLLABORATION, *Mu2e Technical Design Report*, 2015.

BACKUP SLIDES

Charged Lepton Flavour Violation (CLFV)

- **EFT** Lagrangian parametrisation (model-independent): Λ is the effective mass scale and κ controls the relative contribution of the dipole moment term and the four fermion term.

$$\mathcal{L}_{CLFV} = \frac{m_\mu}{(1 + \kappa)\Lambda^2} \bar{\mu}_R \sigma_{\mu\nu} e_L F^{\mu\nu} + \frac{\kappa}{(1 + \kappa)\Lambda^2} \bar{\mu}_L \gamma_\mu e_L \left(\sum_{q=u,d} \bar{q}_L \gamma^\mu \bar{q}_L \right)$$



Possible CLFV models

contenuto terza slide

CLFV experiments

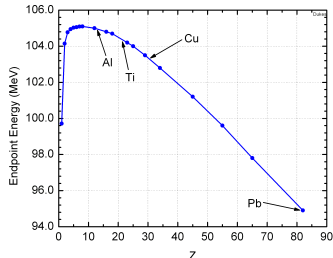
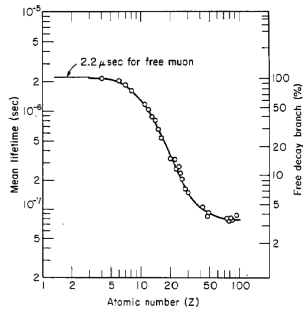
contenuto terza slide

Mu2e beamline

contenuto terza slide

Why Al Stopping Target?

- ▶ Lower RMC background. Photon endpoint: $k_{max} = m_\mu c^2 - |E_b| - E_{rec} - \Delta M$ ~ 101.9 MeV, ~ 3.1 MeV below CE;
- ▶ (Top): quite long lifetime, allowing separation between prompt backgrounds and live window;
- ▶ (Bottom): DIO endpoint dependence on nucleus type. Al \rightarrow high endpoint. Higher- Z nuclei \rightarrow lower endpoint, minimizing background contribution;
- ▶ Conversion BR depends on the ST material. Comparison of conversion BRs on different nuclei normalized to aluminum \rightarrow dominating operator type. Materials with higher Z \rightarrow better model differentiation (Mu2e-II Ti);
- ▶ Available in required size/shape/thickness, low costs and chemically stable.



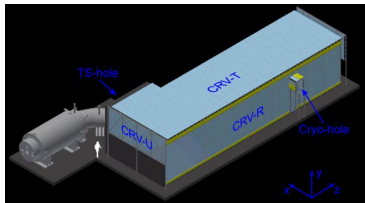
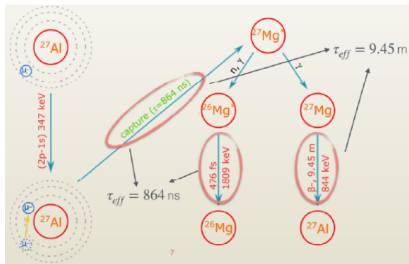
Proton pulses and off spill on spill

Extinction monitor

Cosmic Ray Veto and Stopping Target Monitor

Cosmic Ray Veto:

- ▶ **Active veto:** 4 layers of extruded plastic scintillation counters;
- ▶ **Passive shielding:** Al absorbers between each layer;
- ▶ μ 's signature: 3/4 vetoed.



Stopping Target Monitor:

- ▶ HPGe and LaBr_3 detector → number of μ stopped in ST (10% precision on N_μ);
- ▶ It will measure the photons produced by secondary muonic aluminium orbital transitions (347 keV) and nuclear capture (884 keV, 1809 keV).

Drift tubes

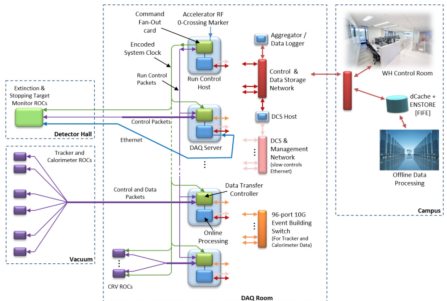
contenuto terza slide

Lorentz effect

contenuto terza slide

DAQ system

- Streaming readout: digitized and zero-suppressed data;
- High data throughput, flexible for analysis;
- DAQ run control via RCH, managing a predefined Run Plan;
- Active spill defined by RF Zero-Crossing Markers from the Accelerator, synced to 1695 ns proton pulses, defining the EW;
- CFO module generates 40 MHz clock, embedding EWMs synced to the system;
- CFO distributes the clock and run control packets to DTCs in DAQ servers;
- DTCs pass the clock to ROCs and EWMs recovered;
- ROCs use EWMs to separate data from consecutive EWs;
- Data Requests trigger ROC data transmission through DTCs post-event;
- EBS routes data from multiple DTCs for online analysis;
- Events logged and transferred to long-term storage (7 PB/year);
- DTCs handle slow control data, managed by DCS Host and stored.

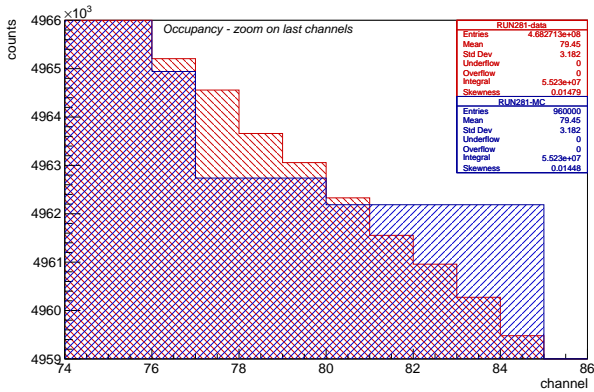


Tracker data format

A **hit data packet** has a fixed length of 256 bits (32 bytes). The packet structure is as follows:

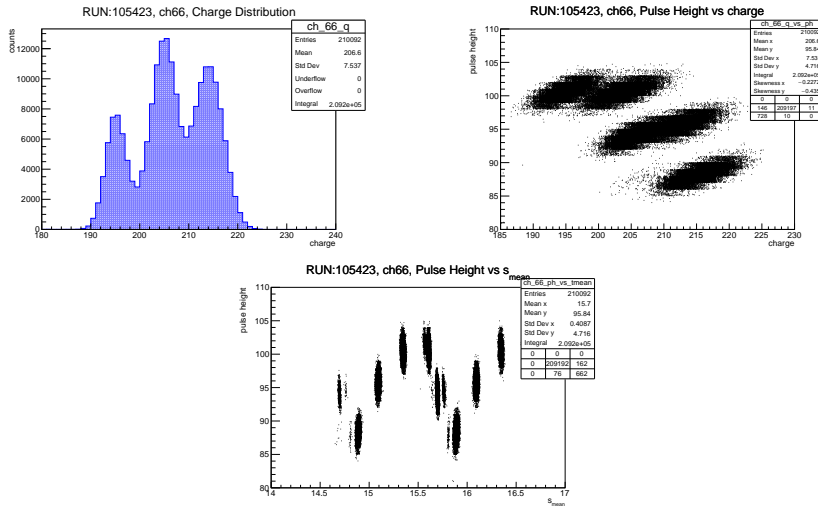
- ▶ 16 bit header (straw index);
- ▶ 16 bit for the TDC left straw end;
- ▶ 16 bit for the TDC right straw end;
- ▶ The ToT (time-over-threshold) values for the two ends of the straw are each stored using 8 bits;
- ▶ The ADC samples require 12 bits each. For each hit, a fixed number of samples (15) is readout;
- ▶ 12 bits are set aside for preprocessing flags.

Additional plots



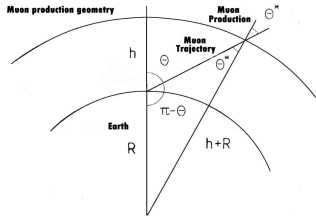
- Zoom on the last readout channels of the occupancy plot.

Additional plots



- ▶ (Left): The (positive) charge distribution of the waveforms (channel 66);
- ▶ (Right): 2D distribution of pulse height versus (positive) charge.

Cosmic muons simulation with CRY



- ▶ CRY (LANL) was used to generate cosmics (straightforward implementation);
- ▶ It simulates protons (1 GeV, 100 TeV), at the top of the atmosphere and generation of muons from the pion decays.
- ▶ It follows Gaisser-Tang model:

$$\frac{dI}{dE_\mu d\Omega dt dS} = \frac{0.14}{\text{cm}^2 \text{ s sr}} \left(\frac{E_\mu}{\text{GeV}} \left(1 + \frac{3.64 \text{ GeV}}{E_\mu (\cos \theta^*)^{1.29}} \right) \right)^{-2.7} \left[\frac{1}{1 + \frac{1.1 E_\mu \cos \theta^*}{115 \text{ GeV}}} + \frac{0.054}{1 + \frac{1.1 E_\mu \cos \theta^*}{850 \text{ GeV}}} \right];$$

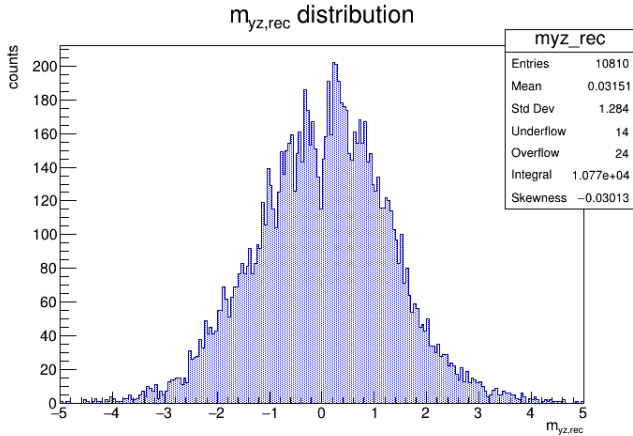
- ▶ $\cos \theta^*$ is given by: $\cos \theta^* = \sqrt{\frac{(\cos \theta)^2 + P_1^2 + P_2(\cos \theta)P_3 + P_4(\cos \theta)P_5}{1 + P_1^2 + P_2 + P_4}}$ with $P_1 \sim 0.10$, $P_2 \sim -0.07$, $P_3 \sim 0.96$, $P_4 \sim 0.04$ and $P_5 \sim 0.82$;
- ▶ (Top): θ^* and θ , zenith angle of muons and at the muon production point.

How to determine channel-to-channel delays

$$\frac{(t_1 + t_2)}{2} = t_d + t_0 + \frac{d_1 + d_2}{2} - \frac{L}{2v}$$

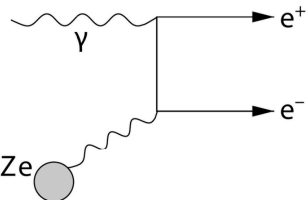
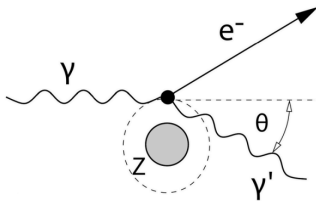
- ▶ $(t_1 + t_2)/2$ allows to measure the drift time up to an offset common to all channels.

Reconstructed muon direction



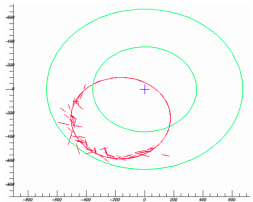
- ▶ Lots of muons reconstructed with $m_{yz} \sim 0$ (horizontal);
- ▶ The true hit position, far from the straws midpoint, results in incorrectly reconstructed tracks' direction on the $y - z$ plane.

δ -electron sources

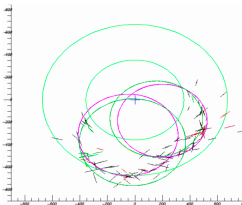


- **Compton scattering:** by γ s interacting with the detector material. Muon capture \rightarrow neutrons \rightarrow neutron capture γ emission ($E_\gamma \sim \text{MeV}$). The Compton effect (Left) is the scattering of a photon by a free or quasi-free ($E_\gamma \gg E_B$) electron. e^-/e^+ asymmetry. Compton cross section per atom proportional to Z ;
- **Pair production** (Right): from nuclear recoil processes. In the Coulomb field of a charge, a photon can convert into an $e^- - e^+$ pair. Z^2 dependence. $E_\gamma \geq 2m_e c^2 + 2\frac{m_e^2}{m_{\text{nucleus}}}c^2$;
- **Delta rays** (or secondary ionization electrons): generated when high-energy charged particles collide with the detector material. A particle collides with shell e^- , resulting in significant energy transfers.

\bar{p} background in Mu2e



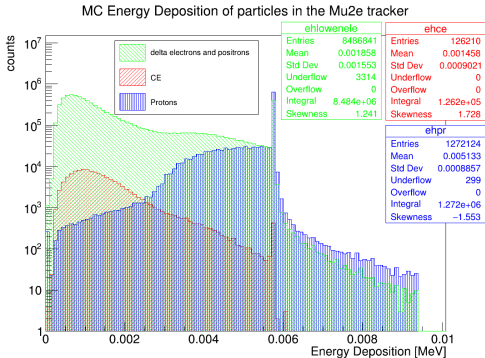
XY view



XY view

- ▶ $\bar{p}s$ are produced from pW interactions;
- ▶ $p\bar{p}$ annihilation at ST $\rightarrow e^-$ by $\pi^0 \rightarrow \gamma\gamma$ followed by γ conversions and $\pi^- \rightarrow \mu^- \bar{\nu}$;
- ▶ The background cannot be suppressed by cuts on the time window because $\bar{p}s$ are slower than other beam particles;
- ▶ There are absorber elements placed in the TS to suppress the $\bar{p}s$;
- ▶ $p\bar{p}$ annihilation at ST can give multiple particle tracks with $p \sim 100$ MeV/c for each track at much higher rate than signal-like;
- ▶ From MC, it was estimated that the rate of such multi-track events is $\times 500$ higher than the rate of events with 1 signal like e^- ;
- ▶ The analysis aims to reconstruct the multi-track final state events and get an estimate of the CE like events by rescaling the two final states ratio.

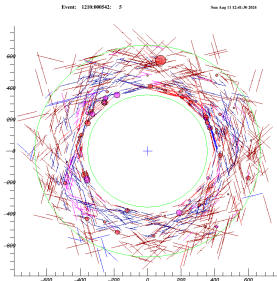
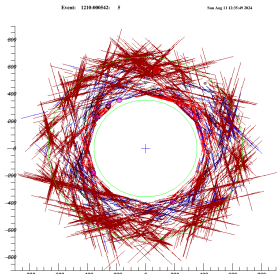
Monte Carlo deposited energy in the tracker



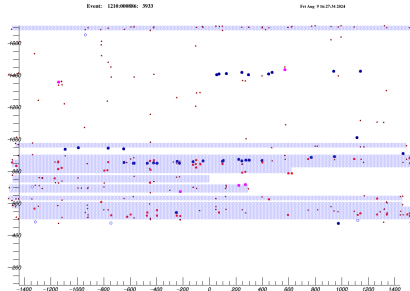
- The Monte Carlo deposited energy distribution in the tracker (*CE – 1BB data sample*);
- (Red) CEs, (green) δ -electrons, (blue) protons.
- Peaks and tails → saturated waveform;
- Only about 4% of CE hits have energies above 3.5 keV (1% above 5 keV);
- Applying an energy threshold in DF can speed up processing, but impacts algorithm efficiency, especially in *seed* reconstruction.

Mu2e event reconstruction

- ▶ Mu2e event reconstruction is optimised to reconstruct single-track events with tracks coming from the ST;
- ▶ Adjacent *StrawHits* within a panel, which are most likely due to the same particle, are combined into a *ComboHit*;
- ▶ δ -electron pre pattern recognition;
- ▶ We cluster the hits within a time window to form *TimeClusters* assuming that such hits are made by the same particle;
- ▶ Hits from *TimeClusters* are used to form helices;
- ▶ Final parameters of the track are determined by the Kalman fit.



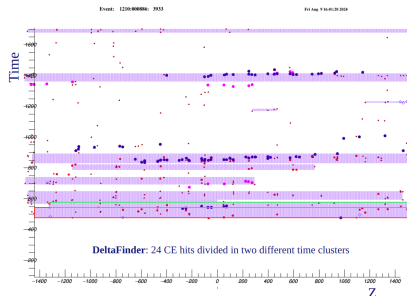
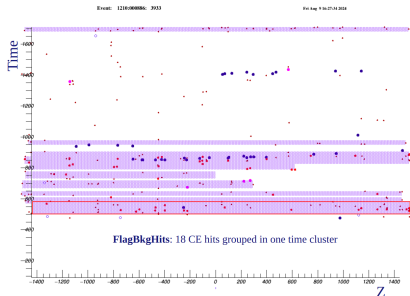
Time Clustering



Time clustering process:

- ① Combination of at least 3 *ComboHits* within a specific $time - z$ window (with a 20 ns time window and a 5-plane z-window);
- ② *Chunks* are created;
- ③ Every potential pair of chunks within a certain time proximity is tested together, and the pair, that minimizes the $\chi^2/ndof$ when the hits are fit to a linear line, is combined;
- ④ Procedure repeated until no further combinations yield a $\chi^2/ndof$ below a set threshold.

Time Clustering development



- ▶ There is a well defined class of events where the effects of hit flaggers get washed out in the reconstruction by the time clustering algorithm;
- ▶ Example:
 - DF: hits from one particle divided in two different time clusters;
 - FBH: not flagged particle hits are used by the time clusterer to *connect* particle hits that are used in the reconstruction. That is why the track is reconstructed in this case.
- ▶ Improving the cluster finder and the pattern recognition could increase the track reconstruction performance.